

## Supporting Information

# A Single Cell Digital Microfluidic Mass Spectrometry Platform for Efficient and Multiplex Genotyping of Circulating Tumor Cells

*Qingyu Ruan<sup>†,‡</sup>, Jian Yang<sup>†,‡</sup>, Fenxiang Zou<sup>†</sup>, Xiaofeng Chen<sup>†</sup>, Qianqian Zhang<sup>†</sup>,  
Kaifeng Zhao<sup>†</sup>, Xiaoye Lin<sup>†</sup>, Xi Zeng<sup>†</sup>, Xiyuan Yu<sup>†</sup>, Lingling Wu<sup>‡,\*</sup>, Shuichao Lin<sup>†,\*</sup>,  
Zhi Zhu<sup>†</sup>, and Chaoyong Yang<sup>†,‡,\*</sup>*

<sup>†</sup> The The MOE Key Laboratory of Spectrochemical Analysis & Instrumentation, the Key Laboratory of Chemical Biology of Fujian Province, State Key Laboratory of Physical Chemistry of Solid Surfaces, Collaborative Innovation Center of Chemistry for Energy Materials, Department of Chemical Biology, College of Chemistry and Chemical Engineering, Xiamen University, Xiamen 361005, China;

<sup>‡</sup> Institute of Molecular Medicine, Renji Hospital, School of Medicine, Shanghai Jiao Tong University, Shanghai 200127, China.

## Table of Contents

### 1. Supporting Experimental Section

1.1. Regents and Materials.....	S4
1.2. Instruments.....	S4
1.3. Cell Culture.....	S4
1.4. Fabrication and Functionalization of DynarFace-Chip.....	S4

### 2. Supporting Figures and Tables

Figure S1. Design of DMF chip for DMF-scMS.....	S6
Figure S2. Schematic illustration of primer extension of a dideoxynucleotide.....	S7
Figure S3. Characterization of DMF-scMS for single-cell isolation at different diameters of hydrophilic spots.....	S8
Figure S4. Single-cell capture efficiency at different cell concentrations.....	S9
Figure S5. Single-cell capture efficiency of DMF-scMS for different chip structures.....	S10
Figure S6. Characterization of DMF-scMS for single-cell isolation from different target cell concentrations.....	S11
Figure S7. Reproducibility of different single cell samples by MALDI-TOF MS detection on the ten hydrophilic spots.....	S12
Figure S8. Schematic illustration of DynarFace-Chip for CTC preenrichment.....	S13
Figure S9. Mass-to-charge ratio peak of parallel MALDI-MS detection of single-CTC samples from patient's blood.....	S14
Figure S10. Schematic summary of the stepwise operation and corresponding time for mutation profiling of single CTCs using DMF-scMS.....	S15
Table S1. The synthesized sequences of primer SNP, SNP-C, SNP-T, SNP-A, and SNP-G.....	S16
Table S2. Sequences of forward, reverse and extension primers of Del19, T790M,	

L858R, C797S, KRAS G12 (34) and KRAS G13 (38) gene.....S17

**Table S3.** Information of blood samples from cancer patients.....S18

**Table S4.** Sequences of forward, reverse and extension primers of colorectal cancer patients.....S19

**Table S5.** The ratio of targeting CTCs successfully genotyped with mutation information.....S20

**Table S6.** Comparison of platforms for oncogenic mutation profiling toward molecular targeted therapies .....S21

### 3. References

## **1. Supporting Experimental Section**

### **1.1 Regents and Materials.**

SU-8-2015 and SU-8-3050 photoresist were supplied by MicroChem (Newton, USA). AZ5214E and AZ4620 were purchased from Clariant AG (Basel, Switzerland). Bovine serum albumin (BSA) was obtained from biofroxx (Einhausen, Germany). Teflon-AF 1600 was obtained from DuPont (Wilmington, USA). Polytetrafluoroethylene emulsion was obtained from Fude Plastics (Dongguan, China). Biotinylated anti-EpCAM antibody was purchased from R&D systems (Minneapolis, USA). EasyTaq DNA Polymerase and DNase/RNase-Free water were purchased from TransGen Biotech (Beijing, China). dideoxyribonucleoside triphosphate (ddNTPs), paraformaldehyde (PFA) powder, ZipTip Micro-C18, ammonium citrate and 3-hydroxypicolinic acid (HPA) were purchased from Sigma-Aldrich (Darmstadt, Germany). Terminator DNA polymerase and shrimp alkaline phosphatase (rSAP) were purchased from New England Biolabs (Beijing, China). REPLI-g Single Cell Kit was purchased from Qiagen (Düsseldorf, Germany). All oligonucleotides used in this work were synthesized and purified by Sangon Biotech (Shanghai, China). All other reagents not mentioned above were purchased from Thermo Fisher Scientific (Grand Island, USA). All chemicals were used without further purification.

### **1.2 Instruments.**

The fluorescence microscope was supplied by Zeiss, Germany. The thermal-cycler for DNA amplification was obtained from Bioer, China. The mass spectrometer was obtained from Zybion Inc., China. DynarFace-Chip was fabricated using the EV Group lithography system (610, Austria). The oxygen-plasma treatment by Alpha Plasma Q150 from Germany. Other instruments used for chip fabrication were supplied in the cleanroom facilities of the Pen-Tung Sah Institute of Micro-Nano Science and Technology, Xiamen University.

### **1.3 Cell Culture.**

All cell lines were cultured at 37 °C under a humidified atmosphere with 5% CO<sub>2</sub>. The non-small-cell lung cancer cell lines A549 and H1975 were grown in Roswell Park Memorial Institute (RPMI) 1640 medium. The colon cancer cell line SW480 was grown in Dulbecco's Modified Eagle Medium. The human embryo lung cell line MRC-5 was cultured in Eagle's Minimum Essential Medium (MEM) with 0.11 g L<sup>-1</sup> sodium pyruvate and 1.5 g L<sup>-1</sup> dicarbonate. All media were supplemented with 10% fetal bovine serum and 1% penicillin-streptomycin before use.

### **1.4 Fabrication and Functionalization of DynarFace-Chip.**

DynarFace-Chip was fabricated according to our reported work.<sup>1</sup> In brief, herringbone chip (HB-Chip) was produced by photolithography with support pillar layer and herringbone structure layer. Both the support pillar layer and herringbone structure layer were 50 μm in height. PDMS replicas were made by pouring PDMS ( $W_{\text{prepolymer}}:W_{\text{crosslinker}} = 10:1$ ) into the molds, degassing by vacuum pump and curing in a drying oven (95 °C, 30 min). After peeling off the PDMS replicas, one inlet and one outlet were punched at the replicas. At last, PDMS replica was bound to a prefab PDMS

slice which was pre-bonded to a clean glass slide after oxygen-plasma treatment, to form the HB-Chip. Immunomagnetic beads (IMBs) was prepared by incubating Dynabeads M-280 streptavidin with anti-EpCAM-Biotin antibody ( $W_{\text{antibody}}:W_{\text{Dynabeads}} = 10 \mu\text{g}:1 \text{ mg}$ ) under rotating mix (room temperature, 30 min). After washing three times with PBS by magnetic separation, IMBs were blocked with 2.5% BSA, and followed by another round of washing. Finally, IMBs were loaded into HB-Chip by manual injection ( $\sim 2.4 \times 10^6$  IMBs per chip) and magnetically attracted into chip substrate by a magnet under chip bottom to form DynarFace-Chip.

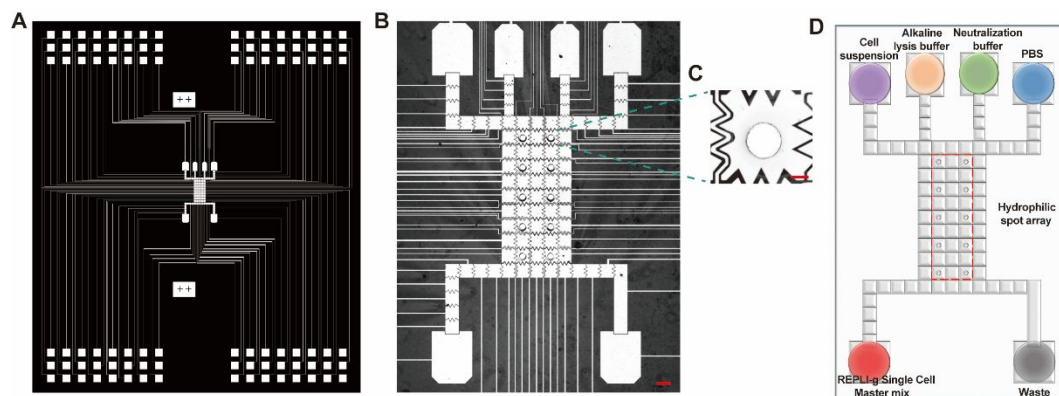


**Figure S1.** Design of DMF chip for DMF-scMS. (A) Computer-aided design of DMF chip. (B) Photograph of the chip made by lithography and wetting. Scale bar, 500  $\mu\text{m}$ . (C) The enlarged view of the hydrophilic spot on the electrode. Scale bar, 100  $\mu\text{m}$ . (D) Schematic diagram of DMF chip with 6 reservoirs for reagent loading, storage and waste as well as an array of hydrophilic spots.

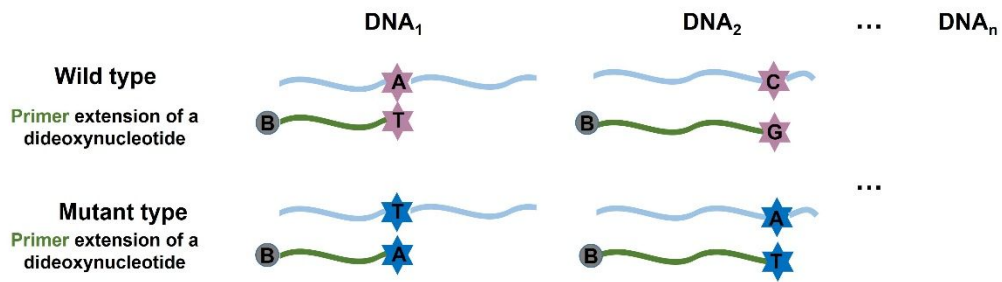


**Figure S2.** Schematic diagram of biotinylated primer (Green) extension of a dideoxynucleotide of target DNA including wild and mutant type.

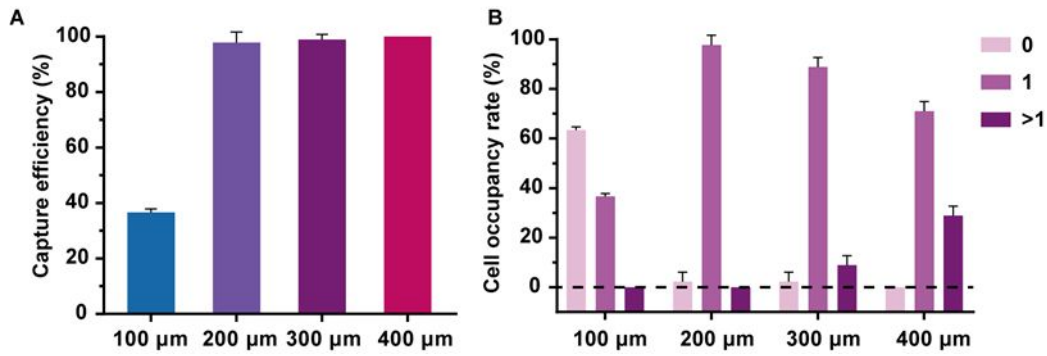


**Figure S3.** Characterization of DMF-scMS for single-cell isolation at different diameters of hydrophilic spots. (A) The relationship between cell capture performance ( $\geq 1$  cell) and the diameters of hydrophilic spots. In the current study, the effect of 100, 200, 300, and 400  $\mu\text{m}$  diameter was investigated under the condition of  $1 \times 10^6$  cells  $\text{mL}^{-1}$ , 120  $\mu\text{m}$  gap and 0.45 mm electrode size. (B) The occupation ratio of no cell, single cell, and more than one cell for different diameters of hydrophilic spots. All data are presented as mean  $\pm$  standard deviation (SD,  $n = 3$ ).

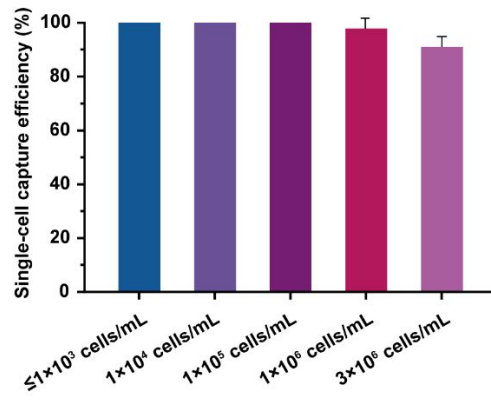


**Figure S4.** Single-cell capture efficiency at different cell concentrations ( $1 \times 10^3$ ,  $1 \times 10^4$ ,  $1 \times 10^5$ ,  $1 \times 10^6$ , and  $3 \times 10^6$  cells  $\text{mL}^{-1}$ ) under the condition of 200  $\mu\text{m}$  hydrophilic spot, 120  $\mu\text{m}$  gap, and 0.45 mm electrode size. All data are presented as mean  $\pm$  SD (n = 3).

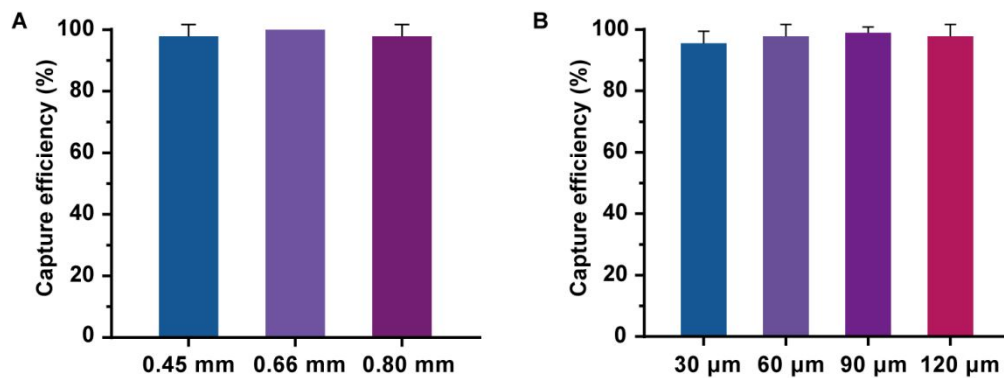


**Figure S5.** Single-cell capture efficiency of DMF-scMS for different chip structures.

Plots showing that the capture efficiency at different lengths of electrode side (A) and various spacer heights (B). For S5A, the single-cell capture efficiency was characterized under the condition of 200 μm hydrophilic spot, 120 μm gap and  $1 \times 10^6$  cells mL<sup>-1</sup>. For S5B, the single-cell capture efficiency was characterized under the condition of 200 μm hydrophilic spot, 0.45 mm electrode size and  $1 \times 10^6$  cells mL<sup>-1</sup>.

All data are presented as mean  $\pm$  SD (n = 3).

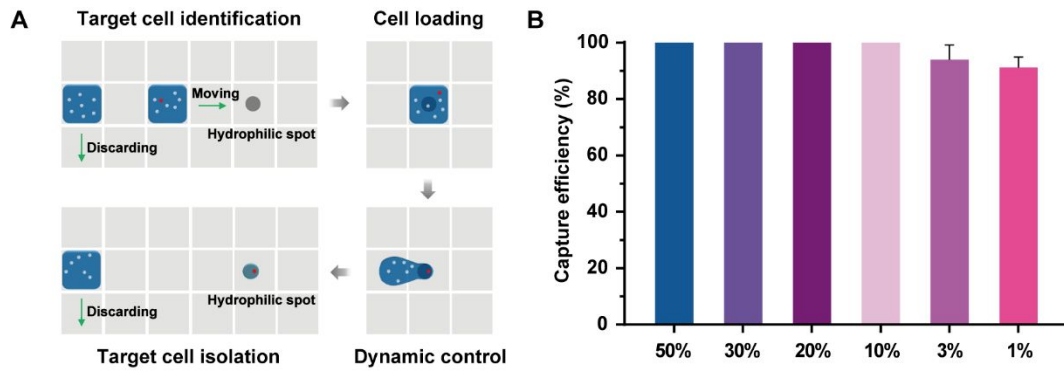


**Figure S6.** Characterization of DMF-scMS for single-cell isolation from different target cell concentrations. (A) Schematic diagram of DMF-scMS for selective capture of single target cell (red) capture from mixed cell populations. (B) Comparison of single target cell capture efficiency of different target cell proportion varying from 50% to 1% of H1975 cells (1%, 3%, 10%, 20%, 30% and 50% H1975 cells mixed with MRC-5 cells with a final cell concentrations of about  $1 \times 10^6$  cells  $\text{mL}^{-1}$ ). All data are presented as mean  $\pm$  SD ( $n = 3$ ).

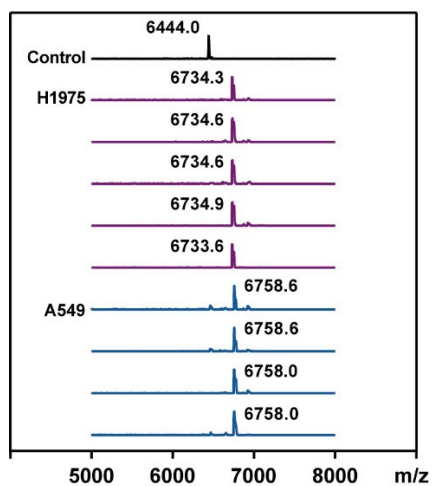


**Figure S7.** Reproducibility of different single cell samples by MALDI-TOF MS detection on the ten hydrophilic spots. One hydrophilic spot captured no cells as a control; each of the five hydrophilic sites captured single H1975 cells; each of the other four hydrophilic sites captured single A549 cells.

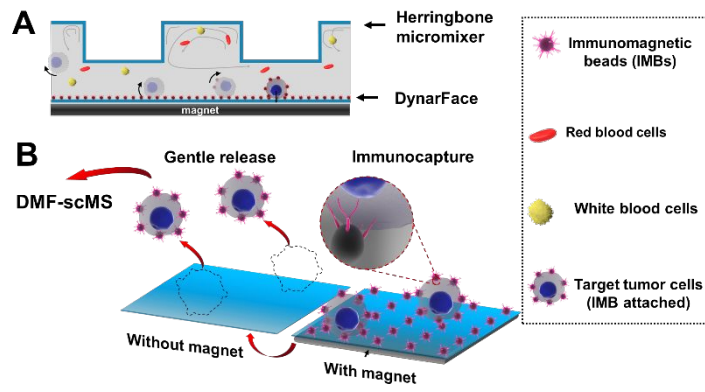


**Figure S8.** (A) The layout of DynarFace-Chip. (B) The schematic diagram for the immunocapture and gentle release of tumor cells using DynarFace-Chip.

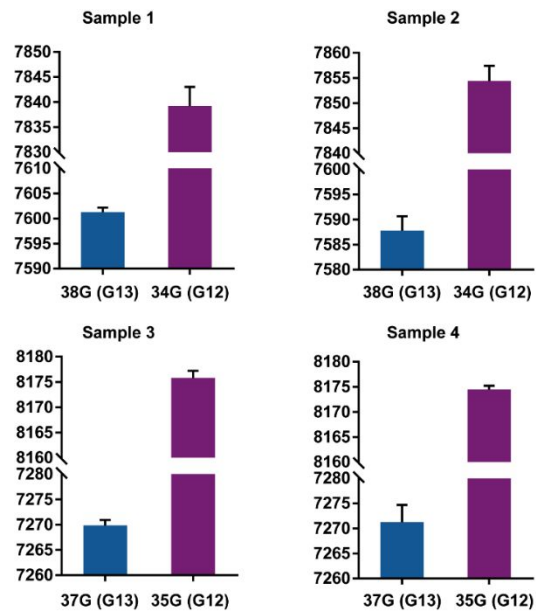


**Figure S9.** Mass-to-charge ratio peak of parallel MALDI-MS detection of single-CTC samples from patient's blood. All data are presented as mean  $\pm$  SD (n = 3).

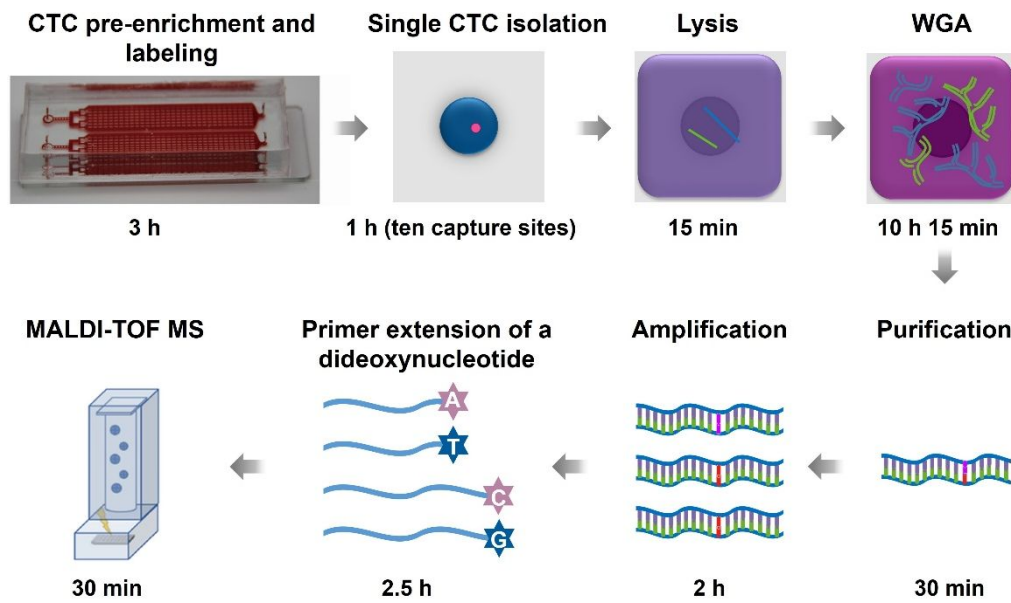


**Figure S10.** Schematic summary of the stepwise operation and corresponding time for gene mutation profiling of single CTCs using DMF-scMS.

**Table S1.** The synthesized DNA sequences of primer SNP, SNP-C, SNP-T, SNP-A, and SNP-G.

SNP primer	5'- CCG CAC CCA GCA GTT TGG CC-3'
SNP primer (T)	5'- CCG CAC CCA GCA GTT TGG CCT-3'
SNP primer (G)	5'- CCG CAC CCA GCA GTT TGG CCG-3'
SNP primer (A)	5'- CCG CAC CCA GCA GTT TGG CCA-3'
SNP primer (C)	5'- CCG CAC CCA GCA GTT TGG CCC-3'

**Table S2.** Sequences of forward, reverse and extension primers of *Del19*, *T790M*, *L858R*, *C797S*, KRAS G12 (34) and KRAS G13 (38) gene.

<b>Del19</b>	<b>Forward</b>	5'-AAC GTC TTC CTT CTC TCT CTG TCA T-3'
	<b>Reverse</b>	5'-CAC ACA GCA AAG CAG AAA CTC AC-3'
	<b>Extension</b>	5'-Biotin-TCC TTG TTG GCT TTC GGA GAT GTT-3'
<b>T790M</b>	<b>Forward</b>	5'-GCC TGC TGG GCA TCT G-3'
	<b>Reverse</b>	5'-TCT TTG TGT TCC CGG ACA TAG TC-3'
	<b>Extension</b>	5'-Biotin-CCG AAG GGC ATG AGC TGC-3'
<b>L858R</b>	<b>Forward</b>	5'-CCC TCA CAG CAG GGT CTT-3'
	<b>Reverse</b>	5'-GTC TGA CCT AAA GCC ACC TC-3'
	<b>Extension</b>	5'-Biotin-CCG CAC CCA GCA GTT TGG CC-3'
<b>C797S</b>	<b>Forward</b>	5'-CCC TCA CAG CAG GGT CTT-3'
	<b>Reverse</b>	5'-GTC TGA CCT AAA GCC ACC TC-3'
	<b>Extension</b>	5'-Biotin-CCG GAC ATA GTC CAG GAG GC-3'
<b>KRAS G12(35)</b>	<b>Forward</b>	5'-TAT AAA CTT GTG GTA GTT GGA GCT-3'
	<b>Reverse</b>	5'-CGT CAA GGC ACT CTT GCC TAC-3'
	<b>Extension</b>	5'-Biotin-ATA AAC TTG TGG TAG TTG GAG CT-3'
<b>KRAS G13(38)</b>	<b>Forward</b>	5'-TAT AAA CTT GTG GTA GTT GGA GCT-3'
	<b>Reverse</b>	5'-CGT CAA GGC ACT CTT GCC TAC-3'
	<b>Extension</b>	5'-Biotin-CTT GTG GTA GTT GGA GCT GGT G-3'

**Table S3.** Blood samples from cancer patients (Clinical investigation by Human KRAS Gene Mutation Detection Kit (Fluorescence PCR method)).

<b>Sample No.</b>	<b>Gender</b>	<b>Age</b>	<b>Clinical investigation</b>	<b>Therapy</b>
<b>1</b>	Male	60	Colon cancer, G12C/R/V/A, or G13C KRAS gene mutation	Surgery
<b>2</b>	Female	62	Rectal cancer, KRAS G12D/S, and G13D mutation	Surgery
<b>3</b>	Female	52	Rectal cancer, G12C/R/V/A, or G13C KRAS gene mutation	Surgery
<b>4</b>	Female	66	Rectal cancer, G12C/R/V/A, or G13C KRAS gene mutation	Surgery
<b>5</b>	Male	64	Rectal cancer, KRAS G12D/S mutation	Surgery

**Table S4.** Sequences of forward, reverse and extension primers of colorectal cancer patients (Primer pair 1 for G12V/A/D and G13C/R/S mutation detection; Primer pair 2 for G12C/R/S and G13D mutation detection).

<b>Primer pair 1</b>	<b>KRAS G12(35)</b>	<b>Forward</b>	5'-TAT AAA CTT GTG GTA GTT GGA GCT-3'
		<b>Reverse</b>	5'-CGT CAA GGC ACT CTT GCC TAC-3'
		<b>Extension</b>	5'-Biotin-ATA AAC TTG TGG TAG TTG GAG CTG-3'
	<b>KRAS G13(37)</b>	<b>Forward</b>	5'-TAT AAA CTT GTG GTA GTT GGA GCT-3'
		<b>Reverse</b>	5'-CGT CAA GGC ACT CTT GCC TAC-3'
		<b>Extension</b>	5'-Biotin-CTT GTG GTA GTT GGA GCT GGT-3'
<b>Primer pair 2</b>	<b>KRAS G12(34)</b>	<b>Forward</b>	5'-TAT AAA CTT GTG GTA GTT GGA GCT-3'
		<b>Reverse</b>	5'-CGT CAA GGC ACT CTT GCC TAC-3'
		<b>Extension</b>	5'-Biotin-ATA AAC TTG TGG TAG TTG GAG CT-3'
	<b>KRAS G13(38)</b>	<b>Forward</b>	5'-TAT AAA CTT GTG GTA GTT GGA GCT-3'
		<b>Reverse</b>	5'-CGT CAA GGC ACT CTT GCC TAC-3'
		<b>Extension</b>	5'-Biotin-CTT GTG GTA GTT GGA GCT GGT G-3'

**Table S5.** The ratio of CTCs successfully genotyped with MS analysis to the total isolated CTCs.

<b>Sample No.</b>	<b>The rate of CTCs genotyped with MS to the total isolated CTCs</b>
<b>Sample 1</b>	2/3
<b>Sample 2</b>	1/3
<b>Sample 3</b>	4/4
<b>Sample 4</b>	4/5

**Table S6.** Comparison of platforms for oncogenic mutation profiling toward molecular targeted therapies.

<b>Platform Name</b>	<b>qPCR for tissue biopsy</b>	<b>NGS for tissue biopsy</b>	<b>DMF-scMS</b>
<b>Accuracy</b>	High	Low	High
<b>Sample source</b>	tissue slice	tissue slice	0.3 mL blood
<b>Sensitivity</b>	> 10 <sup>4</sup> cells	> 10 <sup>4</sup> cells	Single cell
<b>Time cost</b>	4 h	> 7 days	~20 h
<b>Throughput</b>	Several	All	Six key genes
<b>Citation</b>	<i>Small</i> <b>2019</b> , 15, 1805285	<i>Nat. Med.</i> <b>2019</b> , 25, 1415.	This work

**Reference:**

(1) Chen, X.; Ding, H.; Zhang, D.; Zhao, K.; Gao, J.; Lin, B.; Huang, C.; Song, Y.; Zhao, G.; Ma, Y.; Wu, L.; Yang, C., *Adv. Sci.* **2021**, *8*, 2102070.